Conducting Redox Polymer as Organic Anode Material for Polymer-Manganese Secondary Batteries

Kouki Oka,[a, b] Rebecka Löfgren,[b] Rikard Emanuelsson,[b] Hiroyuki Nishide,[a] Kenichi Oyaizu,*[a] Maria Strømme,[b] and Martin Sjödin*[b]

Manganese-based aqueous batteries have attracted significant attention due to their earth-abundant components and low environmental burden. However, state-of-the-art manganese-zinc batteries are poorly rechargeable, owing to dendrite formation on the zinc anode. Organic materials could provide a safe and sustainable replacement. In the present work, a conducting redox polymer (CRP) based on a trimer of EPE (E = 3,4-ethylenedioxythiophene; P = 3,4-propylenedioxythiophene) and a naphthoquinone (NQ) pendant group is used as anode in polymer-manganese secondary batteries. The polymer shows stable redox conversion around + 0.05 V vs. Ag/AgCl, and fast kinetics that involves proton cycling during pendant group redox conversion. For the first time, a CRP-manganese secondary battery was fabricated with pEP(NQ)E as the anode, manganese oxide as the cathode, and manganese-containing acidic aqueous solution as the electrolyte. This battery yielded a discharge voltage of 1.0 V and a discharging capacity of 76 mAh/g_{anode} over > 50 cycles and high rate capabilities (up to 10 C).

1. Introduction

A variety of rechargeable battery technologies have been developed for energy storage to support our current lifestyle. Lead-acid batteries (PbAs)[1] and lithium-ion batteries (LIBs)[2] dominate the market by virtue of their respective strengths. LIBs have a high energy density that meets current demands for portable electronics as well as for electrification of the transport sector while PbAs are low-cost aqueous systems that are easy to scale up for stationary applications. However, LIBs are expensive, raw material extraction and refining is associated with high environmental burden, and it is questionable if LIBs can meet the rapidly increasing demand for electrical energy storage.[2b,3] PbAs, currently make up about half the installed battery capacity, globally. However, the use of lead is linked to several environmental issues including contamination of soil and groundwater with potentially dangerous health impacts and thus its use is restricted by the Restriction on Hazardous Substances (RoHS).[1] Environmentally benign, low cost electrode material for aqueous energy storage system is therefore highly desirable.[4]

Recently, manganese-based aqueous batteries have attracted significant attention due to their earth abundant components, environmental friendliness, low cost, and high theoretical capacity.[5] However, state-of-the-art manganese-zinc batteries show poor cycle life due to the dendrite formation at the zinc anode.[6] Recently, a rechargeable manganese/hydrogen battery, using a platinum/carbon catalyst as an anode, has been reported, which accentuates the possibilities that further research on manganese-based batteries can bring e.g. for grid-scale electrical energy storage.[5a]

Organic materials featuring cheap, earth-abundant, and readily available building blocks with tunable properties have been proposed as a counterpart of inorganic electrode-active materials.[7] Many kinds of organic materials have been investigated to date, e.g. conducting polymers,[8] carbonyl-based compounds[9] and polymers,[10] organosulfur compounds and polymers,[11] and radicals[12] and polymers.[3b,13] By virtue of their good intrinsic conductivity and high charge storage capacity we have proposed the use of conducting redox polymers (CRPs) as an organic electrode materials.[14] In our previous work, the electrochemical characteristics of a CRP based on EPE (E = 3,4-ethylenedioxythiophene; P = 3,4-propylenedioxythiophene) and a naphthoquinone (NQ) pendant group, pEP(NQ)E (p = polymer) (see Scheme 1), were studied in acidic aqueous electrolyte.[14f,15] pEP(NQ)E shows fast and reversible redox conversion that involves proton cycling during pendant group redox conversion around 0.27 V vs. SHE, making it suitable as an anode-active material.

In the current work, pEP(NQ)E has been electrochemically characterized in a manganese-ion containing acidic aqueous electrolyte and a CRP-manganese secondary battery was fabricated utilizing the CRP as anode, manganese oxide (MnO_2)

[a] K. Oka, Prof. H. Nishide, Prof. K. Oyaizu
Department of Applied Chemistry and Research Institute for Science and Engineering
Waseda University
3-4-1 Okubo, Shinjuku, Tokyo 165-8555, Japan
E-mail: oyaizu@waseda.jp

[b] K. Oka, R. Löfgren, Dr. R. Emanuelsson, Prof. M. Strømme, Prof. M. Sjödin
Nanotechnology and Functional Materials, Materials Science and Engineering
The Ångström Laboratory, Uppsala University
Box 534, SE-751 21 Uppsala, Sweden
E-mail: Martin.Sjodin@angstrom.uu.se

Supporting information for this article is available on the WWW under https://doi.org/10.1002/celc.202000711

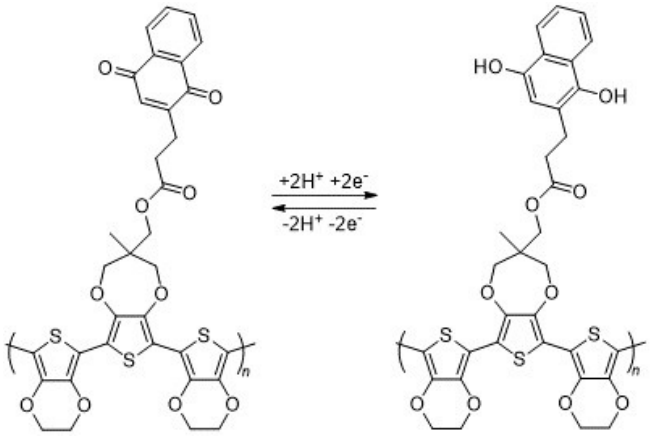

Scheme 1. Redox reaction of pEP(NQ)E.

as cathode, and manganese acidic aqueous solution as electrolyte.

2. Results and Discussion

2.1. Electrochemical Performance of pEP(NQ)E Anode and MnO_2 Cathode

Carbon felts are commonly used as current collectors due to their good electronic conductivity, high stability, and inertness.

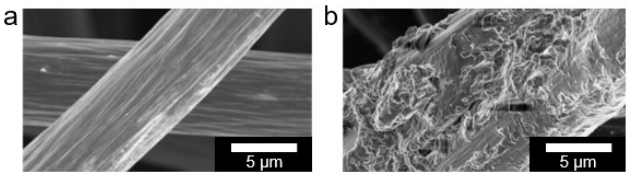

Figure 1. SEM images of pEP(NQ)E electrode. SEM images at 10 000x magnification of a) carbon felt without polymer material and b) carbon felt deposited with polymer material.

They have high porosity which provides easy access to electrolyte ions.[16] In the current work, we prepared pEP(NQ)E on carbon felts as an organic electrode material. The use of carbon felt substrates allowed high mass loadings to be used. SEM analysis of the 10 mg/cm^2 pEP(NQ)E covered carbon felt showed that pEP(NQ)E covered the carbon fiber without forming freestanding aggregates (Figure 1), suggesting a retained pore structure of the felt after polymer deposition albeit with reduced pore size.

While the carbon felt substrate showed a purely capacitive response the pEP(NQ)E covered carbon felt displayed a reversible redox peak at +0.05 V vs. Ag/AgCl in 0.5 M H_2SO_4 aqueous electrolyte (see Figure 2a). This peak has previously been assigned to the $2e^-/2H^+$ redox conversion of the NQ pendant group (see Scheme 1). Reducing-oxidizing (or charge-discharge) curves of the pEP(NQ)E exhibited a voltage plateau at +0.05 V vs. Ag/AgCl, and the coulombic efficiencies (the ratio of discharging vs. charging capacity) were around 100% (Figure S1). The capacity of pEP(NQ)E reached almost the theoretical capacity (76 mAh/g, the capacity estimated from the molecular weight per polymer unit), suggesting that pEP(NQ)E was successfully prepared on carbon felt and almost all the NQ groups contributed to charge storage.

Replacing the 0.5 M H_2SO_4 aqueous electrolyte with a 0.5 M H_2SO_4 + 0.5 M $MnSO_4$ aqueous electrolyte did not significantly change the redox response showing that the NQ redox chemistry is unaffected by the presence of manganese ions and, hence, cycles protons also in the mixed electrolyte. For the half-cell and battery measurements below, we utilized a slightly less acidic electrolyte (1 M $MnSO_4$ + 0.05 M H_2SO_4) to prevent side reactions, such as water oxidation and oxygen evolution. In this case the reversible redox peak is centered at 0 V vs. Ag/AgCl (see Figure 2a). At scan rates below 1 mV/s, the oxidation and reduction peak currents increased linearly with scan rate, suggesting full conversion of the material and a non-diffusion limited reaction at these scan rates. At higher scan rates, above 2 mV/s, the redox peaks moved apart and were broadened, which could be due to sluggish redox conversion of the pendant group (see Figure 2b). From the scan rate dependence

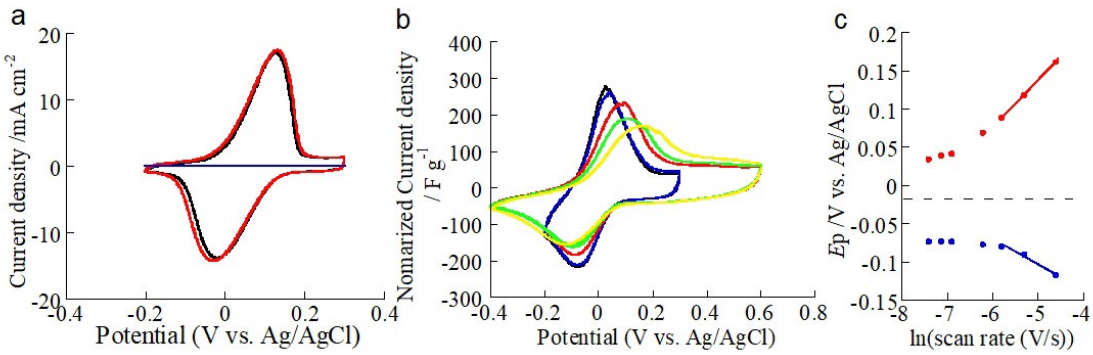

Figure 2. Electrochemical properties and kinetics of pEP(NQ)E. a) Cyclic voltammograms of PEP(NQ)E in 0.5 M H_2SO_4 (black) and 0.5 M $MnSO_4$ and 0.5 M H_2SO_4 (red) aqueous electrolyte, and carbon felt in 0.5 M $MnSO_4$ and 0.5 M H_2SO_4 aqueous electrolyte (blue) at a scan rate of 1 mV/s. b) Cyclic voltammograms of pEP(NQ)E in 1 M $MnSO_4$ and 0.05 M H_2SO_4 aqueous electrolyte at scan rates of 0.6 (black), 1 (blue), 3 (red), 5 (green), and 10 (yellow) mV/s. c) The peak potential dependence on scan rates (0.6, 0.8, 1, 2, 3, 5, and 10 mV/s). Oxidation potentials are red and reduction potentials are blue.

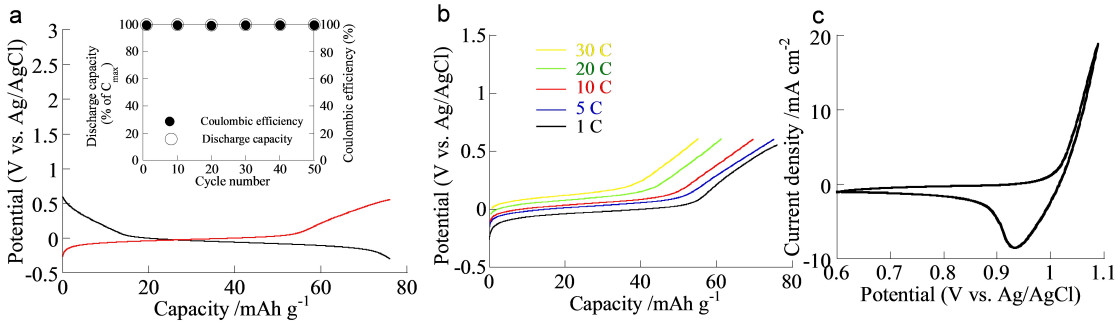

Figure 3. Electrochemical properties of pEP(NQ)E in 1 M $MnSO_4$ + 0.05 M H_2SO_4 aqueous electrolyte. a) The charging (black) and discharging (red) curves of pEP(NQ)E at 10 C. Inset: Capacity retention for 50 cycles upon galvanostatic charge and discharge of pEP(NQ)E at 1 C. b) Discharging curves of the battery at various discharging rates of 1 (black), 5 (blue), 10 (red), 20 (green), and 30 C (yellow). c) Cyclic voltammogram of MnO_2 electrode in 1 M $MnSO_4$ + 0.05 M H_2SO_4

of the peak potentials (Figure 2c), apparent rate constants were calculated[17] to $1.1\times10^{-2}\ s^{-1}$ (oxidation) and $6.8\times10^{-3}\ s^{-1}$ (reduction).

When cycling pEP(NQ)E galvanostatically, a capacity of 76 mAh/g was achieved at 1 C at 0 V vs. Ag/AgCl (Figure 3a). About 99% of the initial capacity was retained during the first 50 cycles at 1 C at a coulombic efficiency 99% (Figure 3a Inset). The rate performance (Figure 3b) of the discharge process showed that all material could be accessed at high C-rates, up to 5 C (720 s discharge time). Furthermore, at 30 C (120 s discharge time), 77% (61 mAh/g) of the theoretical capacity was retained.

The redox reaction at the MnO_2 cathode was evaluated by cyclic voltammetry and the potential of the charge and discharge reactions ($Mn^{2+} + 2H_2O \rightleftarrows MnO_2 + 4H^+ + 2e^-$) was around + 1.0 V vs Ag/AgCl (see Figure 3c). Consequently, combining the pEP(NQ)E anode and MnO_2 cathode, a voltage of 1.0 V in a battery setup could be estimated.

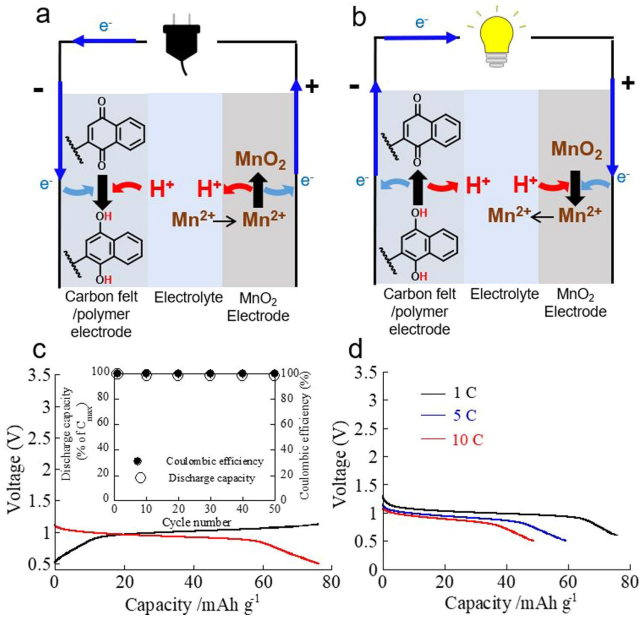

Figure 4. Electrochemical properties of a conductive redox polymer-manganese secondary battery. a) Schematic image of the rechargeable conducting redox polymer-manganese battery (charging). b) Schematic image of the battery (discharging). c) The charging (black) and discharging (red) curves of the battery at 1 C. Inset: Capacity retention for 50 cycles upon galvanostatic charge and discharge of the battery at 1 C. d) Discharging curves of the battery at various discharging rates of 1 (black), 5 (blue), and 10 C (red).

2.2. A CRP-Manganese Secondary Battery

A CRP-manganese secondary battery was fabricated with pEP(NQ)E (almost 10 mg/cm^2 active material) as anode, MnO_2 as cathode, and an aqueous electrolyte containing 1 M $MnSO_4$ and 0.05 M H_2SO_4 (see Figure 4a, 4b). The charging/discharging curves of the cell exhibited a plateau voltage at 1.0 V, and the coulombic efficiencies were almost 100% (Figure 4c). The voltages obtained by this battery corresponded to the potential of pEP(NQ)E against that of Mn^{2+}/MnO_2 ($Mn^{2+} + 2H_2O \rightleftarrows MnO_2 + 4H^+ + 2e^-$). The capacity for the anode used in the device was 76 mAh g^{-1}, suggesting that almost all NQ moieties contributed to charge storage also in the battery cell. The rate performance of the discharge process is shown in Figure 4d. Even at 10 C (360 s discharge time), 64% (49 mAh/g) of the theoretical capacity was retained. The reduced rate performance of the battery compared with that of the pEP(NQ)E itself (Figure 3b) indicates that the MnO_2 cathode is rate limiting. The high capacities (> 98% of the initial capacity) after 50 charging-discharging cycles (Figure 4c Inset) demonstrated a good cycling performance of the CRP-manganese secondary battery, indicating high stability of the CRP anode as well as of the MnO_2 cathode. The battery showed similar cyclability as the previously demonstrated CRP-air battery, using the same anode material,[15] as well as comparable cycling stability with other CRP-based aqueous batteries (Table S1), suggesting that the polymer stability is not affected by the presence of manganese ions in the electrolyte. In addition, the cell shows small resistive losses, as judging from the potential drop between charging and discharging from which a cell resistance was estimated to 8 Ω.

3. Conclusions

A high mass loading (10 mg/cm^2) of the conducting redox polymer electrode was achieved by utilizing a carbon felt as current collector. For the first time, a conducting redox polymer-manganese secondary battery was fabricated with a pEP(NQ)E anode, a MnO_2 cathode, and a 1 M $MnSO_4$ and 0.05 M H_2SO_4 aqueous electrolyte. The battery displayed reversible charging-discharging curves at an output voltage of 1 V, which was close to the potential window of water. Further increase of the mass loading, such as 100 mg/cm^2, is one of the topics of our continuing research.

Experimental Section

Materials

All solvents and chemicals, except *N*-methyl-2-pyrrolidone (NMP), were purchased from Sigma-Aldrich. NMP was purchased from Alfa Aesar Thermo Fisher Scientific. All solvents and chemicals were used without further purifications unless otherwise specified and deionized water was used to prepare aqueous electrolytes. Commercial Soft Graphite Battery Felt AvCarb G200 (thickness 3.2 mm) was purchased from Fuel Cell Store (The surface area of the felt was 3.62 m^2/g from gas adsorption measurement).

Preparation of NQ-EDOT and its Polymerization

The trimer precursor, pEP(NQ)E was synthesized according to the previously published procedures.[14f] Polymerization was achieved by post-deposition-polymerization as follows: First, the NQ-trimer was dissolved in NMP. Thereafter, the trimer solution was soaked into a carbon felt. (The ratio between trimer material and carbon felt used was 10 mg trimer /30 mg (1 cm^2) carbon felt.) The soaked felt was kept in a vacuum chamber for 2 hours to remove NMP. After solvent removal the dry trimer-deposited carbon felt was soaked in electrolyte and shaken for 5 minutes to remove air. Finally, the trimer was electro-polymerized in 0.5 M H_2SO_4 aqueous electrolyte using chronoamperometry for 3000 seconds at 0.6 V, which is well above the onset oxidation potential of trimer (0.2 V vs. Ag/AgCl). After 3000 seconds the polymerization was complete, as judged from the low currents observed. A platinum wire and Ag/AgCl electrode were used as counter- and reference electrode, respectively. Before polymerization the electrolyte was degassed with N_2 for 10 minutes and kept under an inert atmosphere during the measurement.

Preparation of MnO_2 Electrode

The MnO_2 layer was electrodeposited on carbon felt by applying a constant potential of 1.2 V vs. Ag/AgCl in an aqueous electrolyte solution containing 1 M $MnSO_4$ + 0.05 M H_2SO_4 aqueous electrolyte for 200 s.

Electrochemical Characterization

pEP(NQ)E and MnO_2 electrodes were characterized by cyclic voltammetry in aqueous electrolytes. A platinum wire was used as counter electrode and a Ag/AgCl (3 M NaCl, +0.209 V vs. SHE) electrode was used as reference. Electrochemical results were obtained using an Autolab PGSTAT302 N potentiostat (Ecochemie, Utrecht, The Netherlands). The electrolytes were degassed with N_2 and kept under an inert atmosphere during the whole experiment.

Scanning Electron Microscopy

Scanning electron microscopy (SEM) was performed to obtain images of the carbon felt deposited with polymer using a Leo Gemini 1550 FEG SEM (Zeiss, Germany) operated at 3 kV using an in-lens secondary electron detector.

Battery Evaluation

For battery evaluation, a beaker cell was used with the pEP(NQ)E electrode as anode, a MnO_2 on carbon felt as cathode, and 1 M $MnSO_4$ + 0.05 M H_2SO_4 aqueous solution as electrolyte. All battery experiments were carried out under nitrogen atmosphere. The cycling performance of the cell was examined by repeated galvanostatic charging/discharging cycles at 1 C. The cut-off voltages of the pEP(NQ)E/MnO_2 battery were set to 0.5 and 1.2 V. An electrode containing electrodeposited MnO_2 was used as cathode to ensure that the redox reaction occurring at the anode was limiting. The battery was assembled with both anode and cathode in their discharged state.

Acknowledgements

This work was funded through SweGRIDS - by the Swedish Energy Agency, the Carl Trygger Foundation, the Swedish Research Council (VR), the Olle Engqvist Byggmästare Foundation and the Research Council Formas. K.O., H.N., and K.O. acknowledge the financial support by Grants-in-Aids for Scientific Research (17H03072, 18 K19120, 18H03921, 18H05515, 19 J21527) from MEXT, Japan. The collaboration is the direct result of the Top Global University Project from MEXT, Japan.

Conflict of Interest

The authors declare no conflict of interest.

Keywords: conducting redox polymers · organic electronics · renewable energy storage · aqueous manganese batteries · quinones

[1] G. J. May, A. Davidson, B. Monahov, *J. Energy Storage* **2018**, *15*, 145–157.
[2] a) J. B. Goodenough, Y. Kim, *Chem. Mater.* **2010**, *22*, 587–603; b) J. M. Tarascon, M. Armand, *Nature* **2001**, *414*, 359–367.
[3] a) P. Poizot, F. Dolhem, J. Gaubicher, *Current Opinion in Electrochemistry* **2018**, *9*, 70–80; b) H. Nishide, K. Oyaizu, *Science* **2008**, *319*, 737–738.
[4] a) Y. Lu, J. B. Goodenough, Y. Kim, *J. Am. Chem. Soc.* **2011**, *133*, 5756–5759; b) J. Y. Luo, W. J. Cui, P. He, Y. Y. Xia, *Nat. Chem.* **2010**, *2*, 760–765; c) J. O. G. Posada, A. J. R. Rennie, S. P. Villar, V. L. Martins, J. Marinaccio, A. Barnes, C. F. Glover, D. A. Worsley, P. J. Hall, *Renewable Sustainable Energy Rev.* **2017**, *68*, 1174–1182; d) L. M. Suo, O. Borodin, T. Gao, M. Olguin, J. Ho, X. L. Fan, C. Luo, C. S. Wang, K. Xu, *Science* **2015**, *350*, 938–943; e) W. Li, J. R. Dahn, D. S. Wainwright, *Science* **1994**, *264*, 1115–1118; f) H. Kim, J. Hong, K. Y. Park, H. Kim, S. W. Kim, K. Kang, *Chem. Rev.* **2014**, *114*, 11788–11827.
[5] a) W. Chen, G. Li, A. Pei, Y. Li, L. Liao, H. Wang, J. Wan, Z. Liang, G. Chen, H. Zhang, J. Wang, Y. Cui, *Nat. Energy* **2018**, *3*, 428–435; b) K. Zhang, X.

Han, Z. Hu, X. Zhang, Z. Tao, J. Chen, *Chem. Soc. Rev.* **2015**, *44*, 699–728; c) W. Wei, X. Cui, W. Chen, D. G. Ivey, *Chem. Soc. Rev.* **2011**, *40*, 1697–1721.
[6] a) H. Pan, Y. Shao, P. Yan, Y. Cheng, K. S. Han, Z. Nie, C. Wang, J. Yang, X. Li, P. Bhattacharya, K. T. Mueller, J. Liu, *Nat. Energy* **2016**, *1*; b) F. Mo, G. Liang, Q. Meng, Z. Liu, H. Li, J. Fan, C. Zhi, *Energy Environ. Sci.* **2019**, *12*, 706–715.
[7] B. Huskinson, M. P. Marshak, C. Suh, S. Er, M. R. Gerhardt, C. J. Galvin, X. Chen, A. Aspuru-Guzik, R. G. Gordon, M. J. Aziz, *Nature* **2014**, *505*, 195–198.
[8] a) L. M. Zhu, A. W. Lei, Y. L. Cao, X. P. Ai, H. X. Yang, *Chem. Commun. (Camb.)* **2013**, *49*, 567–569; b) F. Goto, K. Abe, K. Ikabayashi, T. Yoshida, H. Morimoto, *J. Power Sources* **1987**, *20*, 243–248.
[9] a) M. Armand, S. Grugeon, H. Vezin, S. Laruelle, P. Ribiere, P. Poizot, J. M. Tarascon, *Nat. Mater.* **2009**, *8*, 120–125; b) Z. Yang, L. Tong, D. P. Tabor, E. S. Beh, M.-A. Goulet, D. De Porcellinis, A. Aspuru-Guzik, R. G. Gordon, M. J. Aziz, *Adv. Energy Mater.* **2018**, *8*.
[10] a) W. Choi, D. Harada, K. Oyaizu, H. Nishide, *J. Am. Chem. Soc.* **2011**, *133*, 19839–19843; b) R. Kato, K. Oka, K. Yoshimasa, M. Nakajima, H. Nishide, K. Oyaizu, *Macromol. Rapid Commun.* **2019**, e1900139; c) S. Maniam, K. Oka, H. Nishide, *MRS Communications* **2017**, *7*, 967–973; d) K. Oka, S. Furukawa, S. Murao, T. Oka, H. Nishide, K. Oyaizu, *Chem. Commun. (Camb.)* **2020**, *56*, 4055–4058.
[11] a) I. Gomez, D. Mantione, O. Leonet, J. A. Blazquez, D. Mecerreyes, *ChemElectroChem* **2018**, *5*, 260–265; b) W. J. Chung, J. J. Griebel, E. T. Kim, H. Yoon, A. G. Simmonds, H. J. Ji, P. T. Dirlam, R. S. Glass, J. J. Wie, N. A. Nguyen, B. W. Guralnick, J. Park, A. Somogyi, P. Theato, M. E. Mackay, Y. E. Sung, K. Char, J. Pyun, *Nat. Chem.* **2013**, *5*, 518–524.
[12] Y. Morita, T. Murata, A. Ueda, C. Yamada, Y. Kanzaki, D. Shiomi, K. Sato, T. Takui, *Bull. Chem. Soc. Jpn.* **2018**, *91*, 922–931.
[13] a) K. Oyaizu, H. Nishide, *Adv. Mater.* **2009**, *21*, 2339–2344; b) S. Muench, A. Wild, C. Friebe, B. Haupler, T. Janoschka, U. S. Schubert, *Chem. Rev.* **2016**, *116*, 9438–9484; c) K. Oyaizu, H. Nishide, in *Conjugated Polymers*, CRC Press, **2019**, pp. 587–594; d) K. Oyaizu, H. Nishide, *Encyclopedia of radicals in chemistry, biology and materials* **2012**; e) H. Nishide, S. Iwasa, Y.-J. Pu, T. Suga, K. Nakahara, M. Satoh, *Electrochim. Acta* **2004**, *50*, 827–831; f) K. Oka, R. Kato, K. Oyaizu, H. Nishide, *Adv. Funct. Mater.* **2018**, *28*.
[14] a) R. Emanuelsson, H. Huang, A. Gogoll, M. Strømme, M. Sjödin, *J. Phys. Chem. C* **2016**, *120*, 21178–21183; b) K. Oka, C. Strietzel, R. Emanuelsson, H. Nishide, K. Oyaizu, M. Strømme, M. Sjödin, *Electrochem. Commun.* **2019**, *105*; c) M. Sterby, R. Emanuelsson, X. Huang, A. Gogoll, M. Strømme, M. Sjödin, *Electrochim. Acta* **2017**, *235*, 356–364; d) C. Karlsson, H. Huang, M. Strømme, A. Gogoll, M. Sjödin, *Electrochim. Acta* **2015**, *179*, 336–342; e) L. Åkerlund, R. Emanuelsson, S. Renault, H. Huang, D. Brandell, M. Strømme, M. Sjödin, *Adv. Energy Mater.* **2017**, *7*; f) C. Strietzel, M. Sterby, H. Huang, M. Strømme, R. Emanuelsson, M. Sjödin, *Angew. Chem. Int. Ed.*, *n/a*.
[15] K. Oka, C. Strietzel, R. Emanuelsson, H. Nishide, K. Oyaizu, M. Strømme, M. Sjödin, *ChemSusChem*.
[16] T. X. Huong Le, M. Bechelany, M. Cretin, *Carbon* **2017**, *122*, 564–591.
[17] E. Laviron, *J. Electroanal. Chem. Interfacial Electrochem.* **1979**, *101*, 19–28.

Manuscript received: May 20, 2020
Revised manuscript received: June 22, 2020
Accepted manuscript online: June 22, 2020